

# Dalton Transactions

Accepted Manuscript

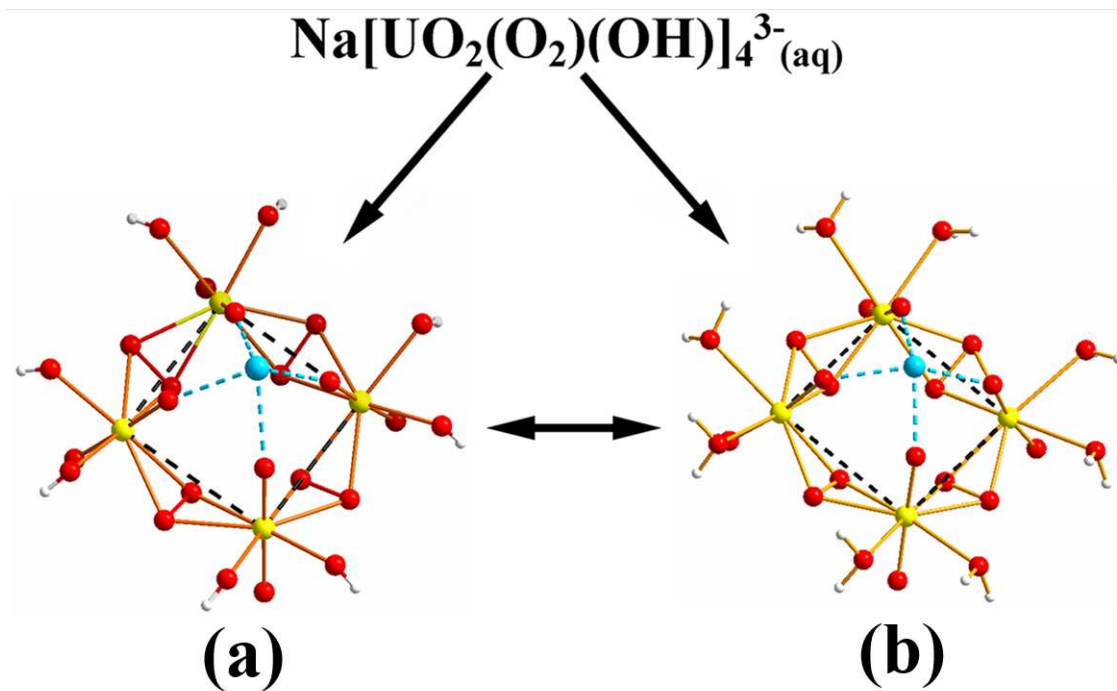


This is an *Accepted Manuscript*, which has been through the Royal Society of Chemistry peer review process and has been accepted for publication.

*Accepted Manuscripts* are published online shortly after acceptance, before technical editing, formatting and proof reading. Using this free service, authors can make their results available to the community, in citable form, before we publish the edited article. We will replace this *Accepted Manuscript* with the edited and formatted *Advance Article* as soon as it is available.

You can find more information about *Accepted Manuscripts* in the [Information for Authors](#).

Please note that technical editing may introduce minor changes to the text and/or graphics, which may alter content. The journal's standard [Terms & Conditions](#) and the [Ethical guidelines](#) still apply. In no event shall the Royal Society of Chemistry be held responsible for any errors or omissions in this *Accepted Manuscript* or any consequences arising from the use of any information it contains.



The complex  $\text{Na}[\text{UO}_2(\text{O}_2)(\text{OH})]_4^{3-}(\text{aq})$  can be modeled by a solid state structure element (a) and by a quantum chemistry using a solvent model (b).

Cite this: DOI: 10.1039/c0xx00000x

www.rsc.org/xxxxxx

ARTICLE TYPE

# Alkali - Metal Ion Coordination in Uranyl(VI) Poly-Peroxide Complexes in Solution. Part 1, The Li<sup>+</sup>, Na<sup>+</sup> and K<sup>+</sup> - Peroxide –Hydroxide Systems.‡

Pier Luigi Zanonato,<sup>a</sup> Plinio Di Bernardo,<sup>\*a</sup>, Valerie Vallet,<sup>b</sup> Zoltán Szabó<sup>c</sup> and Ingmar Grenthe<sup>\*c</sup>

5 Received (in XXX, XXX) Xth XXXXXXXXX 20XX, Accepted Xth XXXXXXXXX 20XX

DOI: 10.1039/b000000x

The alkali metal ions Li<sup>+</sup>, Na<sup>+</sup> and K<sup>+</sup> have a profound influence on the stoichiometry of the complexes formed in uranyl(VI) – peroxide – hydroxide systems, presumably as a result of a templating effect, resulting in the formation of two complexes, M[ $\text{UO}_2(\text{O}_2)\text{OH}$ ]<sub>2</sub><sup>-</sup> where the uranyl units are linked by one peroxide bridge,  $\mu - \eta^2 - \eta^2$ , with the second peroxide coordinated “end-on”,  $\eta^2$ , to one of the uranyl groups, and M[ $\text{UO}_2(\text{O}_2)\text{OH}$ ]<sub>4</sub><sup>3-</sup>, with a four-membered ring of uranyl ions linked by  $\mu - \eta^2 - \eta^2$  peroxide bridges. The stoichiometry and equilibrium constants for the reactions:  $\text{M}^+ + 2\text{UO}_2^{2+} + 2\text{HO}_2^- + 2\text{H}_2\text{O} \rightarrow \text{M}[\text{UO}_2(\text{O}_2)\text{OH}]_2^- + 4\text{H}^+$  (1) and  $\text{M}^+ + 4\text{UO}_2^{2+} + 4\text{HO}_2^- + 4\text{H}_2\text{O} \rightarrow \text{M}[\text{UO}_2(\text{O}_2)\text{OH}]_4^{3-} + 8\text{H}^+$  (2) have been measured at 25 °C in 0.10 M (tetramethyl ammonium/M<sup>+</sup>)NO<sub>3</sub> ionic media using reaction calorimetry. Both reactions are strongly enthalpy driven with large negative entropies of reaction; the observation that  $\Delta H(2) \approx 2\Delta H(1)$ , suggests that the enthalpy of reaction is approximately the same when peroxide is added in bridging and “end-on” positions. The thermodynamic driving force in the reactions is the formation of strong peroxide bridges and the role of M<sup>+</sup> is to provide a pathway with a low activation barrier between the reactants and in this way “guide” them to form peroxide bridged complexes; they play a similar role as in the synthesis of crown-ethers. Quantum chemical methods, (QC), were used to determine the structure of the complexes, and to demonstrate how the size of the M<sup>+</sup>-ions affects their coordination geometry. There are several isomers of Na[ $\text{UO}_2(\text{O}_2)\text{OH}$ ]<sub>2</sub><sup>-</sup> and QC energy calculations show that the ones with a peroxide bridge are substantially more stable than the ones with hydroxide bridges. There are isomers with different coordination sites for Na<sup>+</sup> and the one with coordination to the peroxide bridge and two uranyl oxygen atoms is the most stable one.

## Introduction

We have previously studied the U(VI) – peroxide – hydroxide / fluoride systems both in solution and the solid state<sup>1a, 1c</sup> using tetramethyl ammonium nitrate (TMANO<sub>3</sub>) and NaNO<sub>3</sub> ionic media and noted that the composition of the complexes formed were quite different; in the presence of TMA<sup>+</sup> a mononuclear complex [UO<sub>2</sub>(O<sub>2</sub>)(OH)]<sup>-</sup> was predominant, while complexes with a four or five-membered ring “[UO<sub>2</sub>(O<sub>2</sub>)]<sub>4/5</sub>” was predominant in the fluoride system studied in a NaNO<sub>3</sub> ionic medium. We suggested that the formation of the peroxide bridged polymers was facilitated by Na<sup>+</sup> acting as a template, in much the same way as in the synthesis of crown-ethers.<sup>2</sup> A possible reason for the different stoichiometry in the TMA<sup>+</sup> ionic medium might be the large size of the cation, suggesting that alkali-ions of proper size are necessary for the assembly of ring-shaped complexes. Some support for this is given by the fact that isostructural U-24 phases that contain four-membered rings are formed both in the peroxide/hydroxide and peroxide/fluoride systems in the presence of Na<sup>+</sup>.<sup>1c</sup>

45 A convenient method to study the coordination of alkali-ions would be to use a titration where these ions are added to a test solution that initially contains uranyl, peroxide and hydroxide ions in a TMANO<sub>3</sub> ionic medium. We have shown<sup>1</sup> that solution chemical methods (potentiometry, using p[H<sup>+</sup>] and p[F<sup>-</sup>] selective electrodes, and <sup>17</sup>O and <sup>13</sup>C NMR) can be used to study chemical equilibria in peroxide systems. However, a study of the peroxide/hydroxide system in a mixed TMA<sup>+</sup>/Na<sup>+</sup> medium requires high pH (p[H<sup>+</sup>] > 12), a fact that complicates the experiments because both the decomposition of hydrogen peroxide and the formation of solid phases have to be taken into account; measurements of p[H<sup>+</sup>] are possible, but the sensitivity of glass electrodes is too low to provide data that are sufficiently precise to provide a unique chemical model. Another method to study the coordination of Na<sup>+</sup> in the aqueous peroxide/hydroxide system, would be to use potentiometric titrations where p[Na<sup>+</sup>] concentrations are measured. It turned out that ion-selective sodium electrodes did not work properly at the high p[H<sup>+</sup>] that we had to use and other alternatives had to be tried. We decided to

use calorimetry, in combination with  $^{17}\text{O}$  NMR as the experimental tools, and quantum chemical calculations to provide structures of the complexes and information on reaction thermodynamics, (Gibbs energies, enthalpies and entropies). A description of experimental procedures and the data analysis is given in the Electronic Supporting Information, ESI.<sup>‡</sup>

## Experimental

**Chemicals used.** The same chemicals and preparation methods as in a previous calorimetric study were used.<sup>3</sup> The additional  $\text{NaNO}_3$ ,  $\text{KNO}_3$  and  $\text{LiNO}_3$  were of analytical grade (Aldrich).

**Calorimetric experiments.** The calorimetric study was made using the calorimeter (Thermometric, THAM 2277) at 25 °C, by adding solutions of  $\text{MNO}_3$  ( $\text{M} = \text{Li, Na, K}$ ) to a test solution containing known amounts of uranium, hydrogen peroxide and TMAOH in a 0.100 M  $(\text{TMA})\text{NO}_3$  ionic medium; the experimental procedure for collecting and analyzing the data is described in Ref. 3. Using the software of the system, we measured the heats of reaction and dilution for known additions of titrant and made energy calibrations according to the instrument requirements. In general, we made 30 - 50 additions of titrant during an experiment that lasted from 6 to 9 hours. The stability of hydrogen peroxide, or rather  $\text{HO}_2^-$ , in alkaline solution with and without presence of uranium was investigated in separate experiments. We noted that the Hastalloy assembly of the calorimeter catalyzed the decomposition of hydrogen peroxide and therefore used a glass vessel and tested stirrers made of nylon and glass, only the latter functioned in a satisfactory way and no decomposition of hydrogen peroxide was noted during the course of the experiment. It was necessary to follow a strict protocol when preparing the uranium peroxide solutions in basic medium and to use ratios of  $\text{H}_2\text{O}_2/\text{U}$  close to or higher than one. The heats of dilution determined in separate experiments were very small compared to the heats of reaction.

The compositions of the test solutions are given in Electronic Supporting Information, ESI, Tables S1-S3.

**$^{17}\text{O}$ - NMR spectroscopy.** The test solutions were prepared using  $^{17}\text{O}$  enriched uranyl nitrate, as described in Ref. 1b, hydrogen peroxide and tetramethyl ammonium hydroxide (TMAOH). The initial solution denoted (a), had the composition 10.0 mM uranyl, 70 mM  $\text{H}_2\text{O}_2$  and 70 mM TMA-OH. To this solution we added a solution of 1.00 M NaCl to a concentration of 70 mM in solution (b) and 130 mM in solution (c). Finally solid NaCl was added to a concentration of about 2 M, solution (d). The NMR spectra were recorded using a Bruker DRX-400 spectrometer operating at 0 °C in order to avoid excessive loss of  $\text{O-17}$  enrichment due to exchange with the solvent (75%  $\text{H}_2\text{O}$ , 25 %  $\text{D}_2\text{O}$ ). The experimental data are given in ESI, Table S4 and additional experimental details are given in Ref. 1b, p. 11637.

**Quantum chemical (QC) methods.**

In order to facilitate the quantum chemical calculations we had to use models. The water solvent was described as a dielectric continuum medium and some of the geometry optimizations were made using  $C_n$  symmetry constraints. Solution chemical experiments provide information on the constitution of complexes and their Gibbs energy of reaction. It is straightforward to determine structures using QC methods; this is

not the case for the calculation of reaction energies. Calculation of the enthalpy, entropy and Gibbs energy of reaction requires information on the thermal functions (based on harmonic vibration analysis) of reactants and products, which can only be calculated in the absence of imaginary vibration modes. The structures of all four-membered rings were optimized in the gas phase with the Turbomole quantum chemistry package.<sup>4</sup> However, because of their -1 negative charge, the structures of the uranyl-peroxide dimers were optimized in a continuum polarizable model PCM,<sup>5</sup> which embeds the complex in a molecular shape-adapted cavity (with UFF atomic) interacting with a polarizable continuum medium with the dielectric permittivity of water (80.1). These calculations were made using the Gaussian program<sup>6</sup> as this provides analytical frequencies within the PCM solvent. All geometry optimization were performed at the DFT level with the TPSSH functional,<sup>7</sup> with a ultrafine integration grid, m4, and converging the structure when the Cartesian norm reached  $10^{-4}$  atomic units. The minima were characterized by harmonic vibrational analysis. Uranium was described using a small core pseudopotential (60 core electrons)<sup>8</sup> with the corresponding segmented basis set including a 3 g polarization function,<sup>9</sup> oxygen, hydrogen and all alkali ions were described with aug-cc-pVDZ basis sets.<sup>10</sup> DFT-methods predict geometries fairly accurately, but tend to overestimate binding energies in uranyl complexes. We have checked the performance of the modern suite of M06 functionals (M06L, M06 and M06-2X), and the only one that matches the MP2 accuracy is the M06-2X functional (See ESI, Table S5). However, we have shown in other cases that the MP2 method is more reliable than DFT for describing reaction energies.<sup>11</sup> By using the efficiency of the RI-MP2 technique<sup>12</sup> we made single-point MP2 calculations at the DFT optimized geometries, using larger aug-cc-pVTZ basis sets on the light atoms (for sake of accuracy of the MP2 energy calculations), keeping the 1s core orbitals of oxygen and lithium, the 1s, 2s, and 2p orbitals of sodium, and the 5s, 5p, and 5d orbitals of uranium frozen. The corresponding energies in the water solvent were estimated by a single-point RI-MP2 calculation with the COnductor-like Screening Model (COSMO), for which we used a radius of 1.58 Å that match the  $\text{Na}^+$  free hydration energy better than the default Bondii radius, 1.80 Å.<sup>13</sup>

## Results

**Calorimetric data.** Figure 1 shows the experimental data in the form of the observed stepwise reaction heats as a function of the ratio between the total concentration of  $\text{Na}^+$  and uranium,  $C_{\text{Na}}/C_{\text{U}}$ . The quantitative evaluation of the data was made using the Hyp $\Delta\text{H}$  least-squares program<sup>14</sup> as described in the following.

A general problem with the least-squares analysis of calorimetric data is the correlation<sup>3</sup> between equilibrium constants and the corresponding molar enthalpies of reaction, a fact that had to be considered in the data analysis. The NMR data demonstrated that at least two other species are formed when  $\text{Na}^+$  is added to a solution that initially contains  $[\text{UO}_2(\text{O}_2)(\text{OH})^-]$ ; based on this

observation and on the microcalorimetric results of Figure 1 several models, including such with two and three complexes with formulas  $M[\text{UO}_2(\text{O}_2)(\text{OH})]_n^{1-n}$ ,  $n \leq 4$ , were tested for all the systems analyzed. In all cases, the minimization program excluded formation of the neutral complex  $M[\text{UO}_2(\text{O}_2)(\text{OH})]$  when it was tested together with  $M[\text{UO}_2(\text{O}_2)(\text{OH})]_2^-$  and  $M[\text{UO}_2(\text{O}_2)(\text{OH})]_4^{3-}$ . The same occurred with the trimer,  $M[\text{UO}_2(\text{O}_2)(\text{OH})]_3^{2-}$ . As a result, the best fit in the three systems was obtained with the complexes  $M[\text{UO}_2(\text{O}_2)(\text{OH})]_2^-$  and  $M[\text{UO}_2(\text{O}_2)(\text{OH})]_4^{3-}$ . The analysis of the titration data was made using the least-squares program to optimize the two equilibrium constants and the corresponding enthalpies of reaction. The stability constants and reaction enthalpies of all the complexes not containing the alkali ions and yet necessary to describe the aqueous systems correctly, were maintained fixed at the values shown in ESI, Table S6, during the minimization steps. In general, several steps were used for each system because some of the experimental data suggested the presence of systematic errors. An example is provided by the titrations where the ratio peroxide/uranium  $< 1$  where there is a large concentration of uranyl hydroxide complexes and where even small errors in their enthalpy of reaction (ESI Table S6) can lead to large systematic errors; these titrations were therefore discarded.

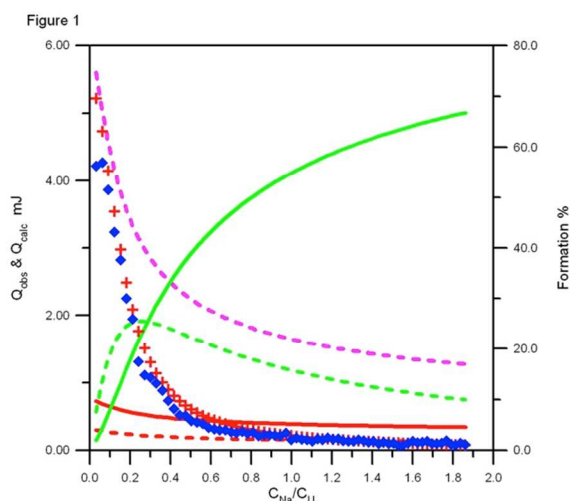
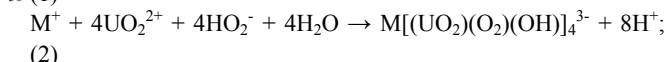
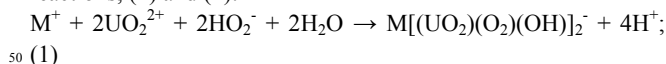


**Figure 1.** A comparison of the stepwise reaction heats (observed, blue diamonds; calculated, red crosses) for titration T3 in the system  $\text{Na}^+ - \text{UO}_2^{2+} - \text{H}_2\text{O}_2 - \text{OH}^-$ . The speciation curves were calculated using the stability constants of Table S6 and those of the selected best model in Table 1. —,  $[(\text{UO}_2)(\text{OH})_3]^-$ ; - - -,  $[(\text{UO}_2)(\text{OH})_4]^{2-}$ ; - - - ,  $[(\text{UO}_2)(\text{O}_2)(\text{OH})]^-$ ; —,  $\text{Na}[\text{UO}_2(\text{O}_2)(\text{OH})]_2^-$ ; - - - ,  $\text{Na}[\text{UO}_2(\text{O}_2)(\text{OH})]_4^{3-}$ .

Titration with the ratio peroxide/uranium  $> 1$  also displayed small systematic deviations between experiment and model, see ESI, but we retained them in the data analysis as they significantly reduce the correlation between the minimized parameters and allow a better estimate of the equilibrium

constants. The uncertainty in the enthalpies of reaction obtained in the least-squares refinements of both equilibrium constants and reaction enthalpies turned out to be unrealistically small, sometimes less than 0.1 kJ/mol. We obtained a more realistic uncertainty by repeating the refinements keeping the  $\log K \pm \sigma$  values constant. The selected equilibrium constants and enthalpies of reaction based on the data in ESI, Tables S1-S3, are reported in Table 1. Comparison of the experimental and calculated heats of reaction for three selected titrations as a function of the ratio  $C_M/C_U$  ( $M = \text{Li}, \text{Na}, \text{K}$ ) is given in ESI, Figures S1 – S3.

The selected chemical model in all three systems includes two reactions, (1) and (2):



The relative amounts of the different complexes during the titration are shown in Figure 1. From the experimental values of reactions (1) and (2) we have calculated the equilibrium constants, enthalpies and entropies of reaction given in Table 1 and noted that the reactions are strongly enthalpy stabilized.

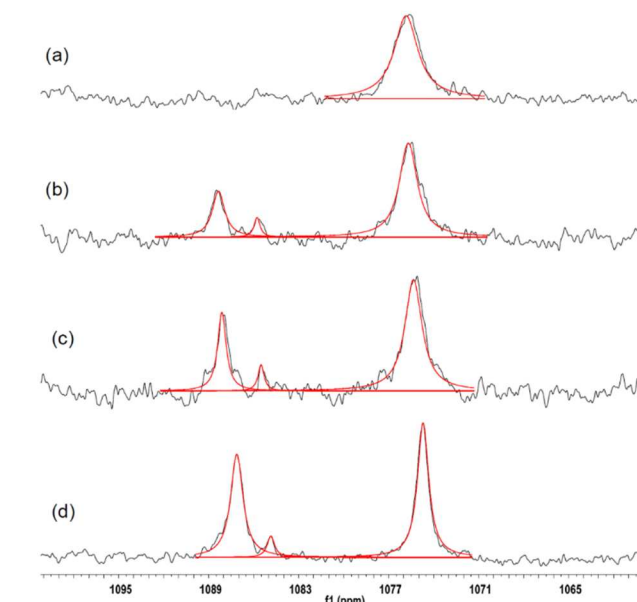
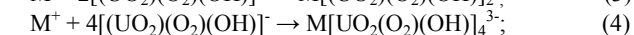
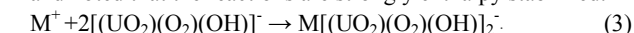
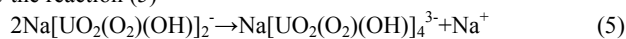


**Figure 2.** (a) The  $^{17}\text{O}$  NMR spectrum of test solution (a) without added  $\text{Na}^+$ ; the predominant complex  $\approx 95\%$  is  $[(\text{UO}_2)(\text{O}_2)(\text{OH})]^-$  located at 1076 ppm. (b) The spectrum of test solution with the concentration of  $\text{NaCl}$  of 70 mM. (c) The spectrum of test solution (c) with  $\text{NaCl}$  concentration of 130 mM. (d) Test solution where solid  $\text{NaCl}$  has been added to a concentration of about 2 M. The peak at 1088 ppm is due to the complex  $\text{Na}[(\text{UO}_2)(\text{O}_2)(\text{OH})]_2^-$  and the peaks at around 1075 ppm to the sum of  $[(\text{UO}_2)(\text{O}_2)(\text{OH})]^-$ ,  $[(\text{UO}_2)(\text{OH})_3]^-$ , and  $\text{Na}[\text{UO}_2(\text{O}_2)(\text{OH})]_4^{3-}$  that have very near the same chemical shifts. The small peak at 1084.5 ppm is probably due to  $\text{Na}[(\text{UO}_2)_2(\text{O}_2)_2(\text{OH})]$  formed from  $[(\text{UO}_2)_2(\text{O}_2)_2(\text{OH})]^-$  and known to be present in small amounts in the absence of  $\text{Na}^+$ .<sup>1a</sup>

*NMR data.*  $^{17}\text{O}$  - NMR spectroscopy. We noticed a significant loss of  $^{17}\text{O}$  enrichment in the solutions tested at 25 °C, presumably due to the presence of  $[(\text{UO}_2)(\text{OH})_3]^-$  by the

<sup>1</sup> In all the systems studied the heat changes decreased suddenly on going from  $C_M/C_U = 0$  to 0.5 and reduced near to zero after that value.

mechanism discussed in one of our previous studies.<sup>15</sup> The <sup>17</sup>O NMR spectra of the different test solutions are shown in Figure 2. The first step in the analysis is to make an assignment of the different peaks in the spectra. There are three prominent complexes in the solution but only two NMR peaks; hence the chemical shifts of two of them must be very near the same. The predominant uranium complex in solution (a) is [(UO<sub>2</sub>(O<sub>2</sub>)(OH))<sub>2</sub>]<sup>-</sup> at 1074 ppm. The spectral changes in solutions (b), (c), and (d) with the appearance of a new peak at 1088 ppm are a result of coordination of Na<sup>+</sup> that increases with increasing concentration of NaCl. The peak at 1085 ppm must be due to Na[(UO<sub>2</sub>(O<sub>2</sub>)(OH))<sub>2</sub>]<sup>-</sup> and the large broad peak around 1075 ppm is then due to the sum of Na[(UO<sub>2</sub>(O<sub>2</sub>)(OH))<sub>4</sub>]<sup>2-</sup> and [(UO<sub>2</sub>(O<sub>2</sub>)(OH))<sub>2</sub>]<sup>-</sup> with very similar chemical shifts. The alternative that the 1085 peak is due to Na[(UO<sub>2</sub>(O<sub>2</sub>)(OH))<sub>4</sub>]<sup>3-</sup> and the 1075 ppm to the sum of Na[(UO<sub>2</sub>(O<sub>2</sub>)(OH))<sub>2</sub>]<sup>-</sup> and [(UO<sub>2</sub>(O<sub>2</sub>)(OH))<sub>2</sub>]<sup>-</sup> would be contrary to the results of the calorimetric experiments. Using the ratio between the 1074 and 1088 ppm peaks we have calculated the equilibrium constants for the reaction (5)



These data are shown in ESI, Table S6. The equilibrium constant  $\log K(5) = 0.1$  at 0 °C is in fair agreement with the value from calorimetry  $\log K(5) = -0.3 \pm 0.3$ , recalculated from the value at 25 °C (Table 1).

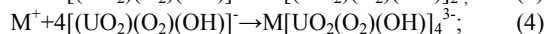
Test solution (d) contains only the two uranyl complexes in Eqn. (5) and the line widths of corresponding NMR peaks, about 1 ppm, show that these are in slow exchange on the NMR time scale. The exchange line-broadening,  $\approx 50\text{Hz}$  corresponds to a residence time of about 6 ms that is the rate of exchange is fast on the time scale used in the calorimetric experiments.

*Quantum chemical data.* Table of coordinates for the various structures investigated are given in the ESI, Table S8 and S9. Details of the various structures will be discussed in the following section

#### Discussion

##### *The Li<sup>+</sup>, Na<sup>+</sup>, and K<sup>+</sup> – uranyl(VI) – peroxide – hydroxide system.*

The most important observations are the transformation of the predominant complex [(UO<sub>2</sub>(O<sub>2</sub>)(OH))<sub>2</sub>]<sup>-</sup> in the initial test solutions in the 0.10 M (TMA)NO<sub>3</sub> medium to M[(UO<sub>2</sub>(O<sub>2</sub>)(OH))<sub>2</sub>]<sup>-</sup> and M[(UO<sub>2</sub>(O<sub>2</sub>)(OH))<sub>4</sub>]<sup>3-</sup> and the very large equilibrium constants for reactions (3) and (4).



The uncertainties in the equilibrium constants given in Table 1 are fairly large due both to experimental difficulties and inherent uncertainties in the least-squares method; nevertheless, the data suggest that the stability constants increase from Li<sup>+</sup> to K<sup>+</sup>. There are large differences between the equilibrium constants and the enthalpy/entropy of reaction between reactions (1) / (2) and (3) / (4). The former have  $K(1)/K(2) \approx 1$  or less, are enthalpy stabilized and entropy disfavored, the latter have large equilibrium constants,  $\log K(3) \approx 5 - 6$  and  $\log K(4) \approx 10 - 11.5$ , which is the result of the very large entropy of reaction; the enthalpy of reaction has small positive values, consistent with the fact that the number of coordinated peroxide ligands is the same between the reactants and the products. The observation that  $\Delta H(2) \approx 2\Delta H(1)$  and  $\Delta S(2) \approx 2\Delta S(1)$ , suggests that the enthalpy and entropy of

reaction is about the same when the peroxide forms a bridge and when it is coordinated to a single uranyl unit. The change in stoichiometry of the complexes when Li<sup>+</sup>, Na<sup>+</sup> or K<sup>+</sup> are added to the aqueous uranyl(VI) – peroxide – hydroxide system demonstrates very clearly the important role of the M<sup>+</sup>-ions in these systems, confirming our suggestion in previous papers.<sup>1</sup>

Their main role is as templates, decreasing the activation barrier between the [(UO<sub>2</sub>(O<sub>2</sub>)(OH))<sub>2</sub>]<sup>-</sup> reactants and in this way “guiding” them to form M[(UO<sub>2</sub>(O<sub>2</sub>)(OH))<sub>n</sub>]<sup>n-</sup>,  $n = 2, 4$ , with peroxide bridges; alkali-ions play a similar role in the synthesis of crown-ethers, where the equilibrium constants for their coordination are small (we have no experimental information on the equilibrium constant for coordination of M<sup>+</sup> to [(UO<sub>2</sub>(O<sub>2</sub>)(OH))<sub>2</sub>]<sup>2-</sup> and [(UO<sub>2</sub>(O<sub>2</sub>)(OH))<sub>4</sub>]<sup>4-</sup>).

An important difference between the ligand rings in the present study and those in crown-ethers is that the former are kinetically labile, and the latter not.

The complex Na[(UO<sub>2</sub>(O<sub>2</sub>)(OH))<sub>4</sub>]<sup>3-</sup> is found as a structure element in [Na<sub>6</sub>(OH<sub>2</sub>)<sub>24</sub>]@[UO<sub>2</sub>(O<sub>2</sub>)(OH))<sub>24</sub>]<sup>18-</sup> (Figure 3) and as shown here in the present study, it is also present in solution, which is a strong indication that it is the precursor for the formation of the U-24 cluster. As there is no evidence for the presence of this in our solutions, we suggest that the cluster is formed in the nucleation / crystallization process.

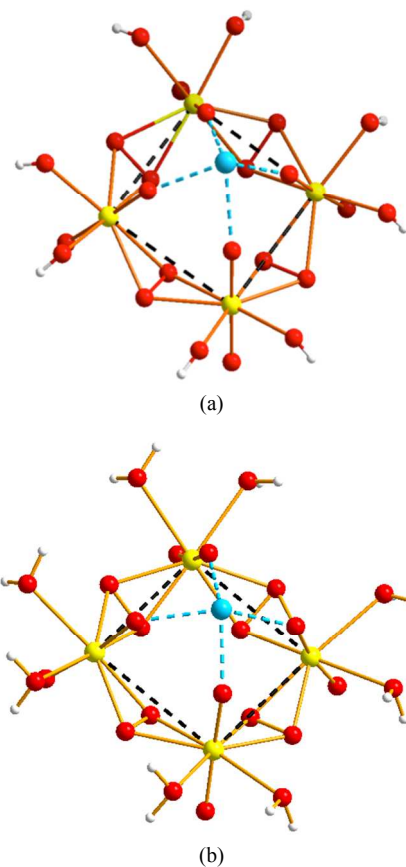


**Figure 3.** (a) Structure of the Na<sup>+</sup>-coordination outside the square faces in [Na<sub>6</sub>(OH<sub>2</sub>)<sub>24</sub>]@[UO<sub>2</sub>(O<sub>2</sub>)(OH))<sub>24</sub>]<sup>18-</sup> from Ref. 1c (note that the hydroxide ions are shared between two uranyl units). There are two non-equivalent uranyl-<sup>17</sup>O<sub>VI</sub> sites in the structure, one with an O<sub>VI</sub> – O<sub>VI</sub> distance of 2.85 Å, to which Na<sup>+</sup> is coordinated, the other at 5.62 Å, too long for Na<sup>+</sup> coordination. (b) Structure of the model Na[(UO<sub>2</sub>(O<sub>2</sub>)(OH))<sub>2</sub>]<sup>4+</sup>

where the hydroxides in structure (a) have been replaced by water molecules.

Solution chemical data do not provide direct structure information on the coordination geometry and the energetics of bonding in the complexes. To obtain this information we have used evidence from QC calculations, using the COSMO model and assuming six-coordination in the equatorial plane of the uranyl group.

The structure and bonding in  $M[(\text{UO}_2)(\text{O}_2)(\text{OH}_2)_2]_4^+$  and  $\text{Na}[(\text{UO}_2)(\text{O}_2)(\text{OH})(\text{OH}_2)_2]_2^{3-}$ . We have used  $M[(\text{UO}_2)(\text{O}_2)(\text{OH})_2]_4^{3-}$  as a QC model for the  $M[(\text{UO}_2)(\text{O}_2)(\text{OH})]_4^{3-}$ ; the structure data in Table 2 for  $\text{Na}[(\text{UO}_2)(\text{O}_2)(\text{OH})]_4^{3-}$  show that this is a good approximation.  $M^+$  is coordinated to four  $\text{O}_{\text{yl}}$  atoms but there are significant changes in these structures when  $M^+$  is changed from  $\text{Li}^+$  to  $\text{Cs}^+$  as shown in Table 2. In the Li-complex the  $\text{O}_{\text{yl}} - \text{O}_{\text{yl}}$  distance in the “ $M(\text{O}_{\text{yl}})_4$ ” unit is significantly shortened, 0.24 Å, as compared to the distance in the complex without coordinated  $M^+$ , while this distance is increased by 0.12 Å in the  $\text{K}^+$  complex and 0.15 Å in the  $\text{Rb}^+$  and  $\text{Cs}^+$  complexes. The  $M^+ - \text{O}_{\text{yl}}$  distances

increases with the ionic radii. The change in the  $\text{O}_{\text{yl}} - M^+ - \text{O}_{\text{yl}}$  angle is very large and decreases from 88.5° in the Li-complex to 65.5° in the Cs-complex. The change in the torsion angle around the peroxide bridge,  $\text{U} - \text{O}_{\text{per}} - \text{O}_{\text{per}} - \text{U}$  is small between all species. There is, however, a significant change in the tilting of the linear uranyl units from the ring plane, in the Li-complexes this angle decreases from 72.5° in the non-coordinated complex to 68.4°, presumably a result of a strong “pull” on the  $\text{O}_{\text{yl}}$  atoms from the small ion. The larger ionic radii in the  $\text{K}^+$ ,  $\text{Rb}^+$  and  $\text{Cs}^+$  complexes result in an increase in the tilt angle to about 73° as the coordinating  $\text{O}_{\text{yl}}$  atoms are pushed apart. We have calculated the energy of distortion from the stable configuration in  $[(\text{UO}_2)(\text{O}_2)(\text{OH})]_4^{4-}$  to the ones in the various complexes by removing the  $M^+$ -ion and then making a single-point energy calculation. The result in Table S7 shows that the distortion energy is the nearly the same,  $11.7 \pm 1.5$  kJ/mol at the MP2 level, in all complexes, suggesting that this is not of major importance for the relative stability of the different  $M[(\text{UO}_2)(\text{O}_2)(\text{OH})]_4^{3-}$  complexes.

**Table 2.** The shortest  $\text{O}_{\text{yl}} - \text{O}_{\text{yl}}$  distance in Å, the angle  $\text{O}_{\text{yl}} - M^+ - \text{O}_{\text{yl}}$  between the cation and two neighboring  $\text{O}_{\text{yl}}$  in degrees, the torsion angle  $\text{U} - \text{O}_{\text{per}} - \text{O}_{\text{per}} - \text{U}$  in the peroxide bridge in degrees and the tilt angle  $\text{U} - \text{U} - \text{O}_{\text{yl}}$  of the linear  $\text{UO}_2$  unit from the ring plane formed by the uranium atoms. The coordinates used are given in ESI, Table S8 and S9 and refer to geometries optimized in the gas-phase.

Complex	$d(\text{O}_{\text{yl}} - \text{O}_{\text{yl}})$ [Å]	$d(M^+ - \text{O}_{\text{yl}})$ [Å]	angle ( $\text{O}_{\text{yl}} - M^+ - \text{O}_{\text{yl}}$ ) [°]	Torsion angle ( $\text{U} - \text{O}_{\text{per}} - \text{O}_{\text{per}} - \text{U}$ ) [°]	Out-of-plane angle $\text{U} - \text{U} - \text{O}_{\text{yl}}$ [°]
$[(\text{UO}_2)(\text{O}_2)(\text{OH}_2)_2]_4$	3.05	-	-	136.1	72.5
$\text{Li}[(\text{UO}_2)(\text{O}_2)(\text{OH}_2)_2]_4^+$	2.81	2.01	88.5	135.3	68.4
$\text{Na}[(\text{UO}_2)(\text{O}_2)(\text{OH}_2)_2]_4^+$	3.07	2.30	83.7	140.0	72.6
$\text{Na}[(\text{UO}_2)(\text{O}_2)(\text{OH})(\text{OH}_2)]_4^{3-}$	3.22	2.28	89.8	144.4	72.3
$\text{K}[(\text{UO}_2)(\text{O}_2)(\text{OH}_2)_2]_4^+$	3.17	2.64	74.8	140.0	73.4
$\text{Rb}[(\text{UO}_2)(\text{O}_2)(\text{OH}_2)_2]_4^+$	3.20	2.81	69.4	140.3	73.5
$\text{Cs}[(\text{UO}_2)(\text{O}_2)(\text{OH}_2)_2]_4^+$	3.20	2.96	65.5	139.9	73.5

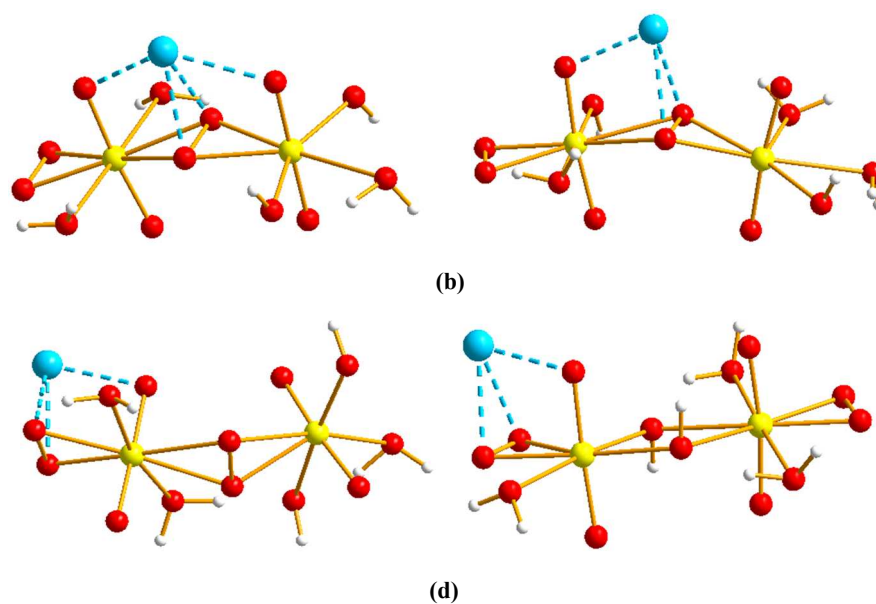


**Figure 4.** Structures of  $\text{Na}[(\text{UO}_2)(\text{O}_2)(\text{OH})(\text{OH}_2)_2]$  isomers (TPSSH-PCM geometries). (a) isomer with the hydroxide ligands coordinated on the same uranyl unit. (b) isomer with coordinated hydroxide on different uranyl units. (c) isomer with coordination of  $\text{Na}^+$  to the terminal peroxide. (d) isomer with coordination of  $\text{Na}^+$  to the terminal peroxide in the hydroxide bridged complex. The inter-atomic distances do not vary much between the different complexes and have not been listed as they are of less importance for the chemical discussion; they can be calculated from the list of coordinates given in ESI, Table S8 and S9.

**Table 3.** Electronic and Gibbs energies of reaction in kJ/mol for different  $\text{Na}[(\text{UO}_2)(\text{O}_2)(\text{OH})_2]^-$  isomers at the MP2 level calculated in a COSMO solvent model. The coordinated water has not been included in the formulae for simplicity.

Isomers	Isomer in Figure 4	$\Delta E$ [kJ/mol]	$\Delta G^\circ$ [kJ/mol]
$\text{Na}_{\text{yl}}[(\text{O}_2)(\text{UO}_2)(\mu\text{-}\eta_2(\text{O}_2))(\text{UO}_2)(\text{OH})_2]^-$	a	0.0	0.0
$\text{Na}_{\text{yl}}[(\text{OH})(\text{O}_2)(\text{UO}_2)(\mu\text{-}\eta_2(\text{O}_2))(\text{UO}_2)(\text{OH})]^-$	b	56.9	62.4
$\text{Na}_{\text{term}}[(\text{O}_2)(\text{UO}_2)(\mu\text{-}\eta_2(\text{O}_2))(\text{UO}_2)(\text{OH})_2]^-$	c	3.2	11.0
$\text{Na}_{\text{term}}[(\text{O}_2)(\text{UO}_2)(\mu\text{-}(\text{OH})_2)(\text{UO}_2)(\text{OH})_2]^-$	d	17.4	31.7

There are several possible isomers of  $\text{M}[(\text{UO}_2)(\text{O}_2)(\text{OH})(\text{OH}_2)_2]^-$  that differ by the bridging ligands, the location of terminal peroxide and hydroxide groups and the coordination of  $\text{M}^+$ . The differences in electronic energy,  $\Delta E$ , and Gibbs energy,  $\Delta G^\circ$ , are given in Table 3. The isomers with two hydroxide on the same uranyl unit (Figure 4a) is 62.4 kJ/mol more stable than the one where they are placed on different ones (Figure 4b), presumably because of a more equal charge distribution. One can also note

35

that the  $\text{Na}^+$  coordination is different in these two isomers, with coordination to four oxygen donors in the one with equal charge distribution (Figure 4a), but only to three in the other isomer (Figure 4b). The isomer where  $\text{Na}^+$  is coordinated to the bridging peroxide (Figure 4a) is the most stable one and the one with coordination to the terminal peroxide (Figure 4c) is less stable by 11.0 kJ/mol. The energy difference is small and within the accuracy of QC energy calculations. The larger stability of the peroxide bridged isomers is also shown by the energy difference between isomers 4c and 4d, where the former is more stable by 10.7 kJ/mol.

*On the nature of the chemical bonding of  $\text{Na}^+$ .* In a previous study<sup>16</sup> we have discussed chemical bonding in uranyl(VI) peroxide complexes and noted that the equatorial bonds are predominantly electrostatic; this is also to be expected for the coordination of  $\text{Na}^+$  to the peroxide and  $\text{O}_{\text{yl}}$  atoms. This is demonstrated in Figure 5, where we show how the electrostatic potential changes when  $\text{Na}^+$  is coordinated to  $[\text{UO}_2(\text{O}_2)(\text{OH})_2]^{2-}$ .

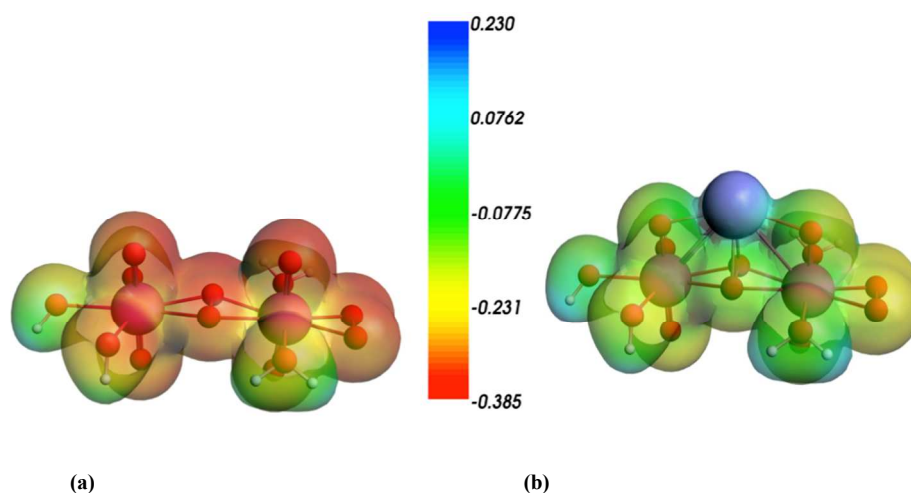


**Figure 5.** (a) Molecular electrostatic potential in  $[(\text{H}_2\text{O})(\text{OH})_2(\text{UO}_2)(\text{O}_2)(\text{UO}_2)(\text{O}_2)(\text{H}_2\text{O})_2]^{2-}$  and (b) in  $[(\text{H}_2\text{O})(\text{OH})_2(\text{UO}_2)(\text{O}_2)(\text{UO}_2)(\text{O}_2)(\text{H}_2\text{O})_2]^-$ . The comparison of the 3D electrostatic potentials in the dimer without and with a bound sodium ion demonstrates that  $\text{Na}^+$ -coordination results in a significant withdrawing of electrons from the electronegative peroxide ligands and the yl-oxygen.

40

## Conclusions.

Addition of alkali-ions to the aqueous uranyl(VI) – peroxide – hydroxide system containing  $[\text{UO}_2(\text{O}_2)(\text{OH})]^-$  results in profound changes in the chemistry. Two new complexes  $\text{M}[(\text{UO}_2)(\text{O}_2)(\text{OH})_2]^-$  and  $\text{M}[(\text{UO}_2)(\text{O}_2)(\text{OH})_4]^{3-}$  ( $\text{M} = \text{Li}, \text{Na}$  and  $\text{K}$ ) are formed and there is no evidence for the formation of other complexes; the two complexes are in the slow exchange regime on the  $^{17}\text{O}$  NMR time-scale. When the reactants are  $\text{UO}_2^{2+}$  and  $\text{HO}_2^-$ , the formation of these complexes are strongly enthalpy driven and the enthalpies of reaction depends mainly on the number of coordinated peroxide ions and less on their location in the complexes, bridging two uranyl units or coordinated to a single one. The equilibrium constants for the formation of  $\text{M}[(\text{UO}_2)(\text{O}_2)(\text{OH})_2]^-$  and  $\text{M}[(\text{UO}_2)(\text{O}_2)(\text{OH})_4]^{3-}$  from

50

$[(\text{UO}_2)(\text{O}_2)(\text{OH})]^-$  are remarkably large and entirely entropy driven; the enthalpy of reaction has small positive values, consistent with the fact that the number of coordinated peroxide ligands is the same between the reactants and the products. The alkali-metal ions act as templates, facilitating the formation of the strong peroxide bridges between the uranyl units that provide the thermodynamic driving force for these reactions. The four-membered ring, “ $\text{Na}[(\text{UO}_2)(\text{O}_2)(\text{OH})_4]^-$ ” is found as a structure element in  $[\text{Na}_6(\text{OH})_{24}]@[(\text{UO}_2)(\text{O}_2)(\text{OH})]_{24}^{18-}$  and other uranyl peroxide clusters.<sup>17</sup> This supports our conclusion in a previous study<sup>2c</sup> that U-24 clusters are formed in the nucleation / crystallization process from a precursor in solution, presumably  $\text{M}[(\text{UO}_2)(\text{O}_2)(\text{OH})_4]^{3-}$ . There are a number of possible structure isomers of structure  $\text{M}[(\text{UO}_2)(\text{O}_2)(\text{OH})_2]^-$  and

55



---

$M[(\text{UO}_2)(\text{O}_2)(\text{OH})]_4^{3-}$  and quantum chemical calculations were used to obtain their structures and relative energies. There is a significant change in the electrostatic potential when  $\text{Na}^+$  is coordinated to  $[(\text{UO}_2)(\text{O}_2)(\text{OH})]_2^{2-}$ , suggesting that the interactions between  $\text{Na}^+$  and the coordinated oxygen donors are essentially electrostatic.

Cite this: DOI: 10.1039/c0xx00000x

www.rsc.org/xxxxxx

## ARTICLE TYPE

**Table 1.** Log's of the equilibrium constants and enthalpies of reaction for the formation of  $M[(\text{UO}_2)(\text{O}_2)(\text{OH})]_2^-$  and  $[(\text{UO}_2)(\text{O}_2)(\text{OH})]_4^{3-}$ ,  $M = \text{Li, Na, and K}$ , and the corresponding quantities for the formation of  $[(\text{UO}_2)(\text{O}_2)(\text{OH})]^-$  from Ref. 3, all at 25 °C in a 0.100 M tetramethyl ammonium nitrate,  $(\text{TMA})\text{NO}_3$ , ionic medium.

Reaction	M	$\log K \pm \sigma$	$\Delta G^\circ \pm \sigma_{\text{est}}$ [kJ/mol]	$\Delta H^\circ \pm \sigma_{\text{est}}$ [kJ/mol]	$\Delta S^\circ \pm \sigma_{\text{est}}$ [ $\text{J K}^{-1} \cdot \text{mol}^{-1}$ ]
$M^+ + 2\text{UO}_2^{2+} + 2\text{HO}_2^- + 2\text{H}_2\text{O} \rightarrow M[(\text{UO}_2)(\text{O}_2)(\text{OH})]_2^- + 4\text{H}^+$ ; (1)	Li	0.0±0.2	0.0±1.1	-78.0±0.2	-262±4
	Na	0.7±0.1	-4.0±0.6	-77.8±0.2	-248±2
	K	0.9±0.2	-5.1±1.1	-85.0±1.0	-268±5
$M^+ + 4\text{UO}_2^{2+} + 4\text{HO}_2^- + 4\text{H}_2\text{O} \rightarrow M[(\text{UO}_2)(\text{O}_2)(\text{OH})]_4^{3-} + 8\text{H}^+$ ; (2)	Li	-0.2±0.3	1.1±1.7	-162.0±0.2	-547±6
	Na	1.0±0.1	-5.7±0.6	-164±3	-530±10
	K	1.3±0.2	-7.4±1.1	-174±8	-560±27
$M^+ + 2[(\text{UO}_2)(\text{O}_2)(\text{OH})]^- \rightarrow M[(\text{UO}_2)(\text{O}_2)(\text{OH})]_2^-$ ; (3)	Li	5.1±0.2	-29.2±1.4	8.8±3.0	127±11
	Na	5.8±0.2	-33.2±1.0	9.0±3.0	142±11
	K	6.0±0.2	-34.4±1.4	1.8±3.2	121±12
$M^+ + 4[(\text{UO}_2)(\text{O}_2)(\text{OH})]^- \rightarrow M[(\text{UO}_2)(\text{O}_2)(\text{OH})]_4^{3-}$ ; (4)	Li	10.0±0.4	-57.3±2.3	11.6±6	231±21
	Na	11.2±0.3	-64.2±1.7	9.6±7	248±24
	K	11.5±0.3	-65.9±2.0	-0.4±10	220±34
$M[(\text{UO}_2)(\text{O}_2)(\text{OH})]_4^{3-} + M^+ \rightarrow 2M[(\text{UO}_2)(\text{O}_2)(\text{OH})]_2^-$ ; (5)	Li	0.2±0.6	-1.1±2.8	6.0±0.4	24±9
	Na	0.4±0.3	-2.3±1.3	8.4±3.0	36±11
	K	0.5±0.5	-2.9±2.5	4.0±8	23±28
$\text{UO}_2^{2+} + \text{HO}_2^- + \text{H}_2\text{O} \rightarrow [(\text{UO}_2)(\text{O}_2)(\text{OH})]^- + 2\text{H}^+$		-2.56±0.07	14.61±0.40	-43.4±1.5	-195±5

Cite this: DOI: 10.1039/c0xx00000x

www.rsc.org/xxxxxx

## ARTICLE TYPE

## Acknowledgements.

P. L. Z. and P. D. B. are grateful for the financial support, grant No. 11217, from the Swedish Nuclear Waste Management Co. (SKB), I. G. for a position as visiting professor from University of Padova and to Mr. Paolo Roverato for technical assistance. V.V is thankful for the support from the French National Research Agency under the contract ANR-11-LABX-0005 Chemical and Physical Properties of the Atmosphere (CaPPA).

## Notes and references

<sup>1</sup> Dipartimento di Scienze Chimiche dell'Università di Padova, Via Marsolo 1, 35131 Padova, Italy.

<sup>b</sup> School of Chemical Sciences and Engineering, Royal Institute of Technology (KTH), S-10044 Stockholm, Sweden.

<sup>c</sup> Université de Lille 1, Laboratoire PhLAM, CNRS UMR 8523, Bât P5, F-59655 Villeneuve d'Ascq Cedex, France.

E-mail: [plinio.dibernardo@unipd.it](mailto:plinio.dibernardo@unipd.it); [ingmarg@kth.se](mailto:ingmarg@kth.se)

‡ Electronic supplementary information (ESI) available: **Tables S1 – S3.**

<sup>20</sup> Composition of solutions used in the calorimetric titrations in the K<sup>+</sup>, Na<sup>+</sup> and Li<sup>+</sup>-uranyl(VI) - peroxide –hydroxide systems. **Table S4.** Test solutions used in the <sup>17</sup>O NMR experiments. **Table S5** Comparison between DFT (M06L, M06, M062X) and MP2 gas-phase energies for Na[(UO<sub>2</sub>)(O<sub>2</sub>)(OH)<sub>2</sub>]<sup>-</sup> isomers. **Table S6** The stability constants and reaction enthalpies of all the complexes involved into the solution equilibria and not containing the alkali ions taken from Ref. 1a. **Table S7.** Distortion energies in the various M[UO<sub>2</sub>((O<sub>2</sub>)(OH)<sub>2</sub>)<sub>4</sub>]<sup>+</sup> complexes. **Table S8.** Cartesian coordinates in Å of the four-membered rings without and with cations (TPSSH gas-phase geometries). **Table S9.** Cartesian coordinates in Å of Na[(UO<sub>2</sub>)(O<sub>2</sub>)(OH)<sub>2</sub>]<sup>-</sup> isomers (TPSSH-PCM geometries). **Figures S1 – S3.** Comparisons of the stepwise reaction heats observed (Qobs) and calculated (Qcalc) for K<sup>+</sup>, Na<sup>+</sup> and Li<sup>+</sup>-uranyl(VI) - peroxide –hydroxide systems.

<sup>35</sup>

- (a) P. L. Zanonato, P. Di Bernardo and I. Grenthe, *Dalton Trans.*, 2012, **41**, 3380–3386. (b) P. L. Zanonato, P. Di Bernardo, Zoltán Szabó and I. Grenthe, *Dalton Trans.*, 2012, **41**, 11635–11648. (c) P. L. Zanonato, P. Di Bernardo, A. Fischer and I. Grenthe, *Dalton Trans.*, 2013, **42**, 10129–10137.
- (a) C. J. Pedersen, *Synthetic Multidentate Macrocyclic Compounds*, pp. 1–51 in R. M. Izatt and J. J. Christensen, Eds. *Synthetic Multidentate Macrocyclic Compounds*, Academic Press, 1978, (b) J. S. Bradshaw, *Synthesis of Multidentate Compounds*, *ibid.* pp. 53–109. (c) N.S. Poonia and A.J. Bajaj, *Chem. Rev.* 1979, **79**, 389–445.
- P. L. Zanonato, P. Di Bernardo and I. Grenthe, *Dalton Trans.* 2014, **43**, 2378–2393.
- TURBOMOLE V6.4 2012, a development of University of Karlsruhe and Forschungszentrum Karlsruhe GmbH, 1989–2007, TURBOMOLE GmbH, since 2007; available from <http://www.turbomole.com>.

- J. Tomasi, B. Mennucci, and R. Cammi, “Quantum mechanical continuum solvation models,” *Chem. Rev.* 2005, **105** 2999–3093.
- Gaussian 09, Revision **D.01**, Frisch, M. J.; Trucks, G. W.; Schlegel, H. B.; Scuseria, G. E.; Robb, M. A.; Cheeseman, J. R.; Scalmani, G.; Barone, V.; Mennucci, B.; Petersson, G. A.; Nakatsuji, H.; Caricato, M.; Li, X.; Hratchian, H. P.; Izmaylov, A. F.; Bloino, J.; Zheng, G.; Sonnenberg, J. L.; Hada, M.; Ehara, M.; Toyota, K.; Fukuda, R.; Hasegawa, J.; Ishida, M.; Nakajima, T.; Honda, Y.; Kitao, O.; Nakai, H.; Vreven, T.; Montgomery, J. A., Jr.; Peralta, J. E.; Ogliaro, F.; Bearpark, M.; Heyd, J. J.; Brothers, E.; Kudin, K. N.; Staroverov, V. N.; Kobayashi, R.; Normand, J.; Raghavachari, K.; Rendell, A.; Burant, J. C.; Iyengar, S. S.; Tomasi, J.; Cossi, M.; Rega, N.; Millam, N. J.; Klene, M.; Knox, J. E.; Cross, J. B.; Bakken, V.; Adamo, C.; Jaramillo, J.; Gomperts, R.; Stratmann, R. E.; Yazyev, O.; Austin, A. J.; Cammi, R.; Pomelli, C.; Ochterski, J. W.; Martin, R. L.; Morokuma, K.; Zakrzewski, V. G.; Voth, G. A.; Salvador, P.; Dannenberg, J. J.; Dapprich, S.; Daniels, A. D.; Farkas, Ö.; Foresman, J. B.; Ortiz, J. V.; Cioslowski, J.; Fox, D. J. Gaussian, Inc., Wallingford CT, 2009.
- Staroverov, V.N., Scuseria, G.E, Tao, J., Perdew, J.P., *J. Chem. Phys.* 2003, **119**, 12129–12137.
- W. Küchle, M. Dolg, H. Stoll, and H. Preuss, *J. Chem. Phys.* 1994, **100**, 7535–7542.
- (a) X. Cao, M. Dolg, and H. Stoll, *J. Chem. Phys.* 2003, **118**, 487–492; (b) X. Cao and M. Dolg, *J. Mol. Struct. (Theochem)*, 2004, **673**, 203–209.
- T.H. Dunning, Jr. *J. Chem. Phys.* 1989, **90**, 1007–1023.
- (a) K. E. Gutowski and D. A. Dixon, *J. Phys. Chem. A*, **2006**, **110**, 8840–8856; (b) P. Wählin, C. Danilo, V. Vallet, F. Réal, J.-P. Flament, and U. Wahlgren, *J. Chem. Theory Comput.* 2008, **4**, 569–577.
- F. Weigend, A and Köhn, C. Hättig, *J. Chem. Phys.* 2002, **116**(8), 3175–3183.
- Tissandier, M. D.; Cowen, K. A.; Feng, W. Y.; Gundlach, E.; Cohen, M. J.; Earhart, A. D.; Coe, J. V. *J. Phys. Chem. A* **1998**, **102**, 7787–7794.
- P.G. Gans, A. Sabatini and A. Vacca, *J. Solution Chem.* 2008, **37**, 467–476.
- (a) Z. Szabó and I. Grenthe, *Inorg. Chem.* 2007, **46**, 9372–9378. (b) Z. Szabó and I. Grenthe, *Inorg. Chem.* 2010, **49**, 4928–4933.
- V. Vallet, U. Wahlgren and I. Grenthe, *J. Phys. Chem A*, 2012, **116**, 12373–12380.
- (a) M. Nyman and P. C. Burns, *Chem. Soc. Rev.* **2012**, **41**, 7314–7367. (b) J. Qui and P. C. Burns, *Chem. Rev.* **2013**, **113**, 1097–1120.